Size optimisation of silver nanoparticles synthesised by gallic acid using the response surface methodology

Mina Ahani, Marziyeh Khatibzadeh ✉

Department of Polymer Engineering and Colour Technology, Amirkabir University of Technology, Tehran 15875-4413, Iran
✉ *E-mail: khatib@aut.ac.ir*

Published in Micro & Nano Letters; Received on 4th January 2020; Revised on 2nd February 2020; Accepted on 14th February 2020

This work reports the synthesis of silver nanoparticles (AgNPs) from Ag nitrate ($AgNO_3$) using the gallic acid (GA) as a green methodology without utilisation of hazardous chemicals. The effects of variables such as $AgNO_3$ concentration, GA concentration, and pH on the average particle size of AgPs were optimised through response surface methodology based on the central composite design at three levels to obtain the desired response, i.e. minimum average particle size. The formation of AgNPs at each experiment was characterised by ultraviolet–visible (UV–vis) spectroscopy and the average particle size was measured by dynamic light scattering (DLS). To evaluate the significance of factors on the response and their quantitative effects, analysis of variance was carried out. The results indicated that the pH was the most effective factor on the response. The AgNPs synthesised at optimised conditions (5.42 mM of AgNO3, 6.25 mM of GA, and pH = 9.02) were characterised by X-ray diffraction, DLS, field-emission scanning electron microscope, energy dispersive X-ray, transmission electron microscopy, UV–vis spectroscopy, and Fourier-transform infrared spectroscopy. On the basis of the DLS, the average particle size of AgNPs obtained 8 nm, which was in satisfactory agreement with the predicted value (7.51 nm) by model.

1. Introduction: Metal nanoparticles (NPs) have gained much attention for a decade due to their outstanding electrical, optical, magnetic, catalytic, and thermal properties as compared with their bulk counterparts, thus opening many possibilities for technological applications [1–3]. These outstanding properties of metal NPs strongly depend on size, shape of NPs, their interactions with capping agents, and surrounding media and also on the manner of their preparation. Therefore, the controllable synthesis of metal NPs is a key challenge to obtain their better-applied characteristics [4]. Among the noble metals, silver NPs (AgNPs) have received considerable attention due to their excellent optical, antimicrobial, and conductive properties, which lead to many potential applications in optics [5], electronic devices [6], antibacterial materials [7], catalysis [8] conductors [9], biosensors [10] etc. A number of different methods have been proposed for the preparation of AgNPs, e.g. physical processes [11], chemical methods of chemical reduction [12], biological [13], water-in-oil microemulsions [14], and green synthesis methods [15–18]. Among the various methods, the chemical reduction method is frequently utilised for the production of AgNPs for the past few years due to its cost-effective, and simplicity. This method is based on reducing Ag salt in an aqueous solution by a reducing agent accompanied by an appropriate capping agent, which is necessary in protecting the growth of Ag particles through aggregation [12]. However, chemical reduction method causes contamination due to utilisation of toxic and hazardous chemicals. Currently, there is a growing need to use environmentally friendly methods for the preparation of NPs that do not produce toxic wastes in their process synthesis. To reduce toxic waste to the environment, researchers have developed 'green' methods [15]. Gallic acid (GA) (3,4,5-trihydroxybenzoic acid), a naturally occurring low molecular weight triphenolic compound, is abundant in many of plants, such as gallnut, green tea, oak bark, red wine, and white wine and fruits, such as banana, strawberry, and grape. GA has been extensively used as antioxidants in food, and as derivate in colour, cosmetic, and pharmaceutical formulations [19, 20]. GA has been also used in the green synthesis of AgNPs [19] because GA is water soluble and is found to be very strong reducing and capping agent for reduction of Ag ions into AgNPs in synthesis process. In the green synthesis of AgNPs by GA, a rigorous control of the different process factors such as pH, type, amount, and order of addition of reactants, allows control of the size, shape, and size distribution of the particles. Conventionally, the effect of these factors has been investigated by performing experiments, in which one of the factors is varied maintaining the other factors fixed at constant levels. Jamdagni *et al.* [21] studied the optimisation of synthesis parameters to assess optimum conditions for green synthesis of AgNPs by 'one factor at a time' method. They represented that the synthesis parameters, such as time, metal ion concentration, reducing agent quantity, reaction temperature, and pH affect the final product and obtained the optimum conditions for synthesis of AgNPs. Generally, the 'one factor at a time' method requires a huge number of experimental runs to determine optimal conditions, which is laborious, time consuming, and ignoring interaction effects between the considered factors [22]. The limitations of the conventional method can be avoided by employing the response surface methodology (RSM) that is an effective tool for optimising the process and studying the effect of several factors influencing the responses by varying these factors simultaneously [23]. RSM is performed adjusting first- or second-order polynomial equations to the experimental data obtained in an experimental design such as the central composite design (CCD) to describe the behaviour of variables. Then, the results obtained by CCD were analysed by analysis of variance (ANOVA). The developed model can also be plotted in three-dimensional (3D) response surface graph that corresponds to response function used for better understanding of the effects of the variables on the response and as well as determination of the optimised conditions of a process [24]. We have recently investigated optimisation of effective parameters in the preparation of AgNPs based on the polyol process (the reduction of Ag salt by ethylene glycol in the [the presence of poly(vinyl pyrrolidone)] by statistical experimental design. As a result, a statistical design of experiment can be preferred to decrease the number of experiments, while considering the interaction between variables [25]. The present Letter is a novel approach involving the optimisation of process variables, i.e. determining the optimised values of variables [Ag nitrate ($AgNO_3$) concentration, GA concentration, and pH] in the green synthesis of AgNPs by GA as both reducing and capping agent using statistical experimental design in order to obtain the desired response, i.e. minimum average particle size. In this respect, a CCD was applied for statistical design of the experiments to

evaluate the coefficients in a quadratic mathematical model. Then, RSM was used to predict the optimised conditions in production of AgNPs. The formation of NPs at each experiment was characterised by UV–vis spectroscopy and the average particle size of synthesised Ag was measured by dynamic light scattering (DLS) analysis. The optimised synthesis conditions have been determined according to RSM and the synthesised AgNPs at these conditions are investigated through analyses of the X-ray diffraction (XRD), DLS, field-emission scanning electron microscope (FE-SEM), energy dispersive X-ray (EDX), transmission electron microscopy (TEM), UV–vis spectroscopy, and Fourier-transform infrared spectroscopy (FT-IR).

2. Experimental results

2.1. Materials and synthesis of AgNPs: $AgNO_3$ (purity 99.9%) as an Ag source, GA ($C_7H_6O_5$) as both reducing and capping agent, and sodium hydroxide (NaOH) for adjusting pH value were obtained from Merck Chemicals, Germany and used as purchased. Deionised (DI) water for the preparation of solutions obtained from Zolal Company, Iran.

At first, aqueous solution of $AgNO_3$ and GA were prepared at a certain concentration, separately. AgNPs were prepared by dropping the GA solution into the $AgNO_3$ solution slowly. After all solutions were added, the mixed solutions were stirred for 5 min. Then, 1 M solution of NaOH was added dropwise until a desired pH was reached. After adjusting the pH value, the obtained mixture was stirred at 25°C for 30 min.

2.2. Characterisation: In all experiments, formation of AgNPs was confirmed by a UV–vis spectrophotometer (JENWAY-6715, UK) operated at a resolution of 1 nm and in the range of 300–800 nm with DI water as a reference.

The average particle size of synthesised particles was measured by DLS for all of samples prepared according to experimental conditions determined by CCD (see Table 1). DLS measurements were conducted with a Malvern Zetasizer Nanoseries instrument (Malvern Instruments Ltd., Malvern, UK) at 25°C.

The synthesised AgNPs at optimised conditions were investigated through analyses of the XRD, DLS, FE-SEM, EDX, UV–vis spectroscopy, and FT-IR. Resulting AgNPs solution was centrifuged at 9000 rpm for 30 min. The solid residues of AgNPs were washed twice with DI water and then redissolved in absolute ethanol. Finally, it was dried by evaporating at 80°C to obtain the powder of the AgNPs for XRD measurement. The XRD analysis was conducted by a Bruker AXS: D8 ADVANCE diffractometer, using monochromatic copper (Cu) kα radiation ($\lambda = 1.5406$ Å) operated at a voltage of 40 kV and 30 mA current in the 2θ range of 5–80°. The size and morphology of synthesised particles were determined using FE-SEM (Mira TESCAN) operating at an acceleration voltage of 15 kV. Specimen of AgNPs for FE-SEM measurement was prepared by drying a drop of Ag colloid deposited onto an aluminium grid at room temperature. The presence of elemental Ag was determined using EDX analysis. EDX measurement was performed on a SUPRA55 (Carl Zeiss, Germany) instrument coupled to the FE-SEM. The TEM image was acquired using a transmission electron microscope (Zeiss-EM10C-80KV) after placing the diluted colloidal solution onto a carbon-coated Cu grid followed by drying the sample. The FT-IR spectra of the samples were measured on a Bomem Hartman & Braun FT-IR spectrophotometer by making a potassium bromide pellet with AgNPs solution. Measurements were made in the range of middle infrared of 4000–400 cm^{-1} at a resolution of 4 cm^{-1} with the use of 20 scans.

2.3. Experimental design and optimisation: Experimental design generally applied to optimise the influencing factors in a process to improve characteristics performance and minimise experimental errors. It is beneficial to determine the most important factors with minimum number of experiments [23]. One of the most important experimental design techniques used in developing, improving, and optimising of processes is RSM. This method consists of a collection of statistical and mathematical techniques used to design experiments, build models, evaluate the effects of variables, and searching optimal conditions of variables to predict targeted responses. Its greatest applications particularly have been in situations where a large number of variables influencing the system feature [26]. This design procedure involves four important steps, namely doing statistically designed experiments for measurement of the response, developing mathematical model of second order with the best fittings, determining the optimal set of experimental factors that produce optimal value of response, and representing the direct and interactive effects of factors by graphical plots [27]. Among the second-order models most used in analytical procedures, CCD has been widely applied in different scientific areas.

In the present Letter, a three-level CCD under RSM developed by Minitab version 16 (Minitab, Inc., USA) was applied to evaluate the significance of the effects of three factors including $AgNO_3$ concentration, GA concentration, and pH that lead to performing the 20 experiments for the optimisation process. The original values of each factor and their corresponding levels are shown in Table 2. The development of the experiments according to the CCD as well as the obtained responses (average particle size) is listed in Table 1.

The correlation of the variables and the response was calculated by a quadratic polynomial equation as shown below:

$$Y = \beta_0 + \beta_1 A + \beta_2 B + \beta_3 C + \beta_{11} A^2 + \beta_{22} B^2 + \beta_{33} C^2 + \beta_{12} AB + \beta_{13} AC + \beta_{23} BC \quad (1)$$

where Y is the predicted response (average particle size); A, B, and C are the coded independent variables; β_0 is the regression coefficient at centre point; β_1, β_2, and β_3 are the linear coefficients; β_{11}, β_{22}, and β_{33} are the quadratic coefficients; and β_{12}, β_{13}, and

Table 1 CCD experiments and obtained responses

Run number	A	B	C	Observed average particle size, nm
1	5	7	9	8.28
2	3	5	11	43.50
3	7	5	7	43.37
4	7	9	11	52.90
5	3	9	7	52.00
6	5	7	9	8.28
7	3	5	7	46.00
8	7	9	7	48.50
9	3	9	11	55.00
10	5	7	9	9.00
11	7	5	11	41.00
12	5	7	9	8.50
13	5	7	9	8.50
14	5	5	9	9.38
15	7	7	9	10.00
16	5	7	7	38.00
17	5	9	9	19.18
18	5	7	9	9.00
19	3	7	9	12.86
20	5	7	11	39.00

Table 2 Values and levels of factors in the experimental design

Process variable	Symbol	Coded levels		
		−1	0	1
$AgNO_3$ concentration, mM	A	3	5	7
GA concentration, mM	B	5	7	9
pH	C	7	9	11

doi: 10.1049/mnl.2019.0780

β_{23} are the interaction coefficients. The statistical significance of the constructed model was evaluated by F-test and P-value in ANOVA. Values of P-value <0.05 show that the factors are significant. The quality of the fit polynomial model was explained by the coefficient of determination R^2. A high R^2 value close to 1.0 confirms the accuracy of the predicted model. After the determination of optimised conditions by RSM, AgNPs were synthesised at these conditions to validate the predicted model.

3. Results and discussion

3.1. UV–visible spectral analysis: After the synthesis, the presence of AgNPs at each experiment was confirmed using UV–vis spectroscopy in the range of 300–800 nm, which has been identified as a very useful method for the analysis of NPs. The surface plasmon resonance (SPR) spectra of synthesised particles in Fig. 1 revealed an absorption peak at the 388–395 nm wavelength range, which corresponds to AgNPs production [28].

3.2. Optimisation of process variables: In all runs, after the addition of the GA solution to the aqueous solution of $AgNO_3$ and adjusting of pH value, at ambient temperature, the colour of the reaction mixture changed from colourless to dark yellowish brown. The change in colour indicates the presence of AgNPs in solution [15]. Operation conditions are known to affect the time required to change the colour of the solution (rate of formation of the NPs) and the intensity of colour (quantity of synthesised NPs). So, optimisation of the process variables is necessary to attain the optimal conditions in the synthesis of AgNPs. In this process, three variables including $AgNO_3$ concentration, GA concentration, and pH were selected. After performing the experiments designed according to the experimental design, the average particle size for each experiment was determined by DLS analysis, which was spotted as the response. The results of experiments are represented in the last column of Table 1. In the next step, for evaluating the relationship between process variables and response, a second-order polynomial model (2) was proposed to calculate the optimised levels of process variables. By applying multiple regression analysis to experimental data, the second-order polynomial equation was obtained

$$Y = 723.453 - 8.733A - 21.953B - 138.469\,C + 0.773A^2 + 1.485B^2 + 7.540C^2 - 0.015A\,B + 0.048A\,C + 0.383B\,C \quad (2)$$

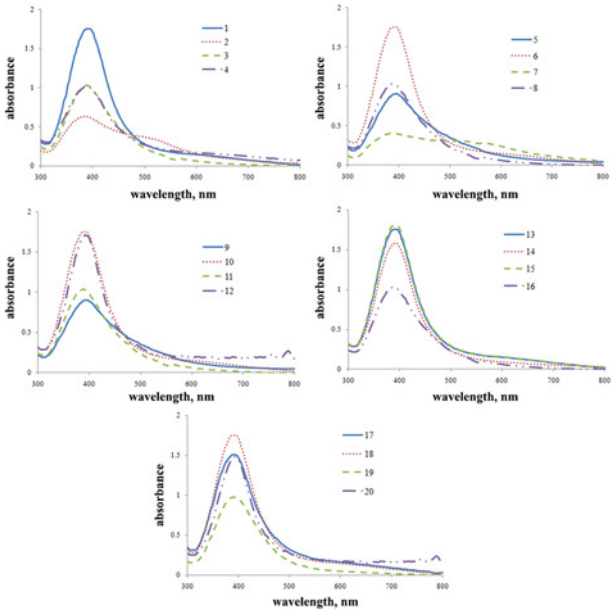

Fig. 1 *UV–vis absorption spectra of the synthesised AgNPs*

where Y was the predicted response and A, B, and C were the coded values of $AgNO_3$ concentration, GA concentration, and pH, respectively. Fig. 2 draws the experimental values of average particle size with the calculated from equation ones together. The R-square value of 0.9998 for the synthesis of AgNPs in Fig. 2 indicates good agreement between the experimental and calculated values to confirm the reliability of the applied model. The significance and adequacy of the constructed model were checked through the ANOVA using F-test and P-value (Table 3). The model F-value of 4244.50 and P-value of <0.0001 for AgNPs synthesis imply that the model is statistically significant in determining the particle size of synthesised Ag. According to Table 3, the linear factors (A, B, and C), the quadratic factors (A^2, B^2, and C^2) and the interaction factor (BC) were found significant (p<0.05). The other factors (AB and AC) were not significant to the response (p > 0.05).

The interaction effects and optimal levels of the factors were studied by plotting the 3D response surface curves when one of the factors is fixed at the optimal value and the other two are allowed to vary. Therefore, three response surface curves (shown in Figs. 3*a–c*) were obtained by considering all the possible combinations. Fig. 3*a* represents the interaction between $AgNO_3$ concentration and GA concentration at fixed value of the pH equal to 9.02. It clearly shows a slight decrease in average particle size of AgNPs with the increase of $AgNO_3$ concentration from 3 to 5.42 mM and GA concentration from 5 to 6.25 mM; further increase in the $AgNO_3$ and GA concentrations led to gradual increase in average particle size. This plot shows a weak degree of curvature at two sides; hence, there was no significant interaction between both factors. It also shows that the minimum response can be achieved when $AgNO_3$ and GA concentrations at the values of 5.42 and 6.25 mM, respectively. Fig. 3*b* represents the interaction between $AgNO_3$ concentration and pH at fixed GA concentration

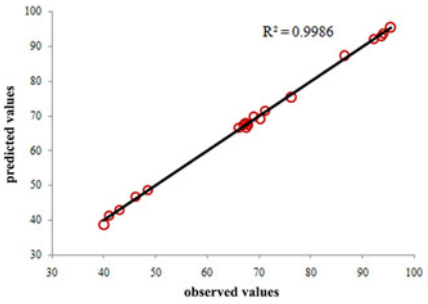

Fig. 2 *Parity plot for the experimental and predicted values of average particle size of AgNPs*

Table 3 ANOVA for CCD

Source of variation	Sum of squares	Degree of freedom	Mean square	F-value	P-value
model	5472.36	9	608.04	4244.50	0.000
A	22.64	1	22.64	158.04	0.000
B	88.97	1	88.97	621.07	0.000
C	2353.40	1	2353.40	16,428.20	0.000
A^2	25.64	1	25.64	178.98	0.000
B^2	94.73	1	94.73	661.26	0.000
C^2	2441.72	1	2441.72	17,044.73	0.000
AB	0.03	1	0.03	0.19	0.672
AC	0.29	1	0.29	2.04	0.191
BC	18.82	1	18.82	131.37	0.000
lack of fit	0.90	5	0.18	2.15	0.281
pure error	0.25	3	0.08	—	—
total	6773.47	19	—	—	—

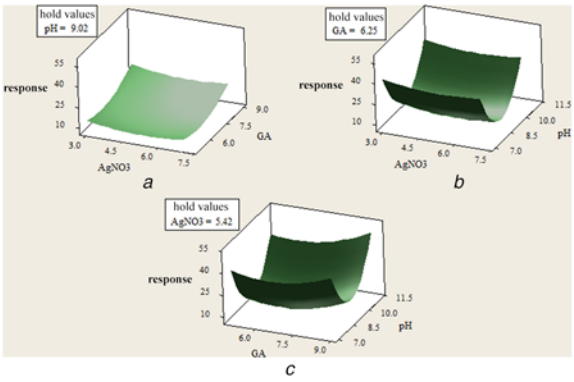

Fig. 3 *Response surface curves for the CCD*
a $AgNO_3$ concentration–GA concentration
b $AgNO_3$ concentration–pH
c GA concentration–pH

of 6.25 mM. It clearly exhibits a strong and weak degree of curvature for pH and $AgNO_3$ concentration, respectively. From the response surface plot, it is obvious that pH had a significant effect on average particle size compared with other factors and the optimal levels for $AgNO_3$ concentration and pH are obtained as 5.42 mM and 9.02, respectively. Fig. 3*c* shows the 3D response surface plot at varying GA concentration and pH at fixed $AgNO_3$ concentration of 5.42 mM. A minimum average particle size can be observed in Fig. 3*c*, which corresponds to a GA concentration of 6.25 mM and pH of 9.02. In this figure, it observes a strong and slightly strong degree of curvature for pH and GA concentration, respectively, implying that the average particle size was significantly affected by pH and GA concentration, where pH produces greater effect. These results are in agreement with those obtained by statistical ANOVA results.

Our results confirmed the very important role played by pH in controlling the size of the AgNPs synthesis. Sathishkumar *et al.* [29] reported that the pH plays a major role in size control of the particles; large particles were formed at lower pH, whereas highly dispersed, small particles were formed at high pH. Therefore, the particles size decreased with the increase of the pH value up to 9 due to the increase of the reduction rate of the Ag ions (more nucleation). The average particle size increases when the pH value is further increased to 11. The increase in particle size is related to aggregation of particles due to the very rapid reduction of Ag ions and the formation particles with very small sizes. So, an optimum pH of 9 has been determined based on our studies. Concerning GA concentration effect, our results show that it was also an effective factor on the average particle size. GA acts as a reducing and capping agent, the oxidation reaction of phenol groups in GA was responsible for the reduction of Ag ions, and the produced quinoid compound with a carboxylic acid group could be adsorbed on the surface of AgNPs accounting for their stabilisation through electrostatic stabilisation (see Fig. 4) [30]. At low GA concentration, the compound is not able to completely cover the Ag ions and reduction rate is also slow; consequently, agglomerated and large particles are produced. The smaller average particle size could be achieved with the increase in the GA concentration to the optimal value (6.25 mM) due to the higher stabilisation of produced particles by GA. Further increases in the GA concentration led to enlarge of average particle size, because it increases the reduction rate too much, and GA is not able to completely cover all of the produced Ag ions; thus, the size of the particles increases. The optimal GA concentration provided the conditions required to produce particles with a sufficiently small average particle size. The next factor investigated was the $AgNO_3$ concentration, which is a slightly significant factor, and it effects on the nucleation process of NPs. As the $AgNO_3$

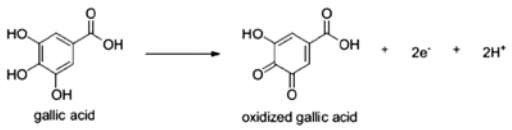

Fig. 4 *Two-electron oxidation of GA to corresponding quinoid compound [30]*

concentration increased from 3 to 5.42 mM, the formation of AgNPs also increased (more nuclei with smaller sizes); however, it was found that increasing the $AgNO_3$ concentration from 5.42 to 7 mM caused the growth of crystals around the nucleus, resulting in an increase in average particle size. Finally, the optimal conditions for synthesis of AgNPs with the minimum average particle size were found in $A = 5.42$ mM, $B = 6.25$ mM, and $C = 9.02$ and at these conditions, the predicted value of Y (average particle size) was 7.51 nm.

3.3. Validation of the predicted model: To determine the correctness of the variance analysis model, sets of experiments were performed by selecting pH and GA concentration as two factors, which have a more major influence on average particle size compared with $AgNO_3$ concentration. The remaining factor in these experiments was at fixed level: $AgNO_3$ concentration (5.42 mM). Table 4 summarises the average particle size of each individual experiment along with the predicted response by model, where the results verify the previous model that 6.25 mM concentration of GA and pH of 9 as the best combination for obtaining the minimum average particle size. The minimum average particle size of 8 nm (Table 4) was obtained experimentally and this was closer to the predicted value (7.51 nm).

3.4. Green synthesis of AgNPs at optimised conditions and characterisation: One experiment at the optimised conditions was performed to verify the reliability of predicted model. Fig. 5 shows the XRD pattern for the AgNPs synthesised at optimised conditions, which clearly indicates the formation of the Ag crystalline structure. Four strong diffraction peaks at 38.53°, 44.53°, 64.83°, and 77.90° can be attributed to the (111), (200), (220), and (311) crystalline structures of the face-centred cubic (FCC) Ag, respectively (identified by ref: 01-087-0719), whereas any peaks originating from Ag oxides cannot be observed. Furthermore, the average crystallite size of NPs was 4.5 nm, was calculated by well known Scherrer equation.

The particle size distribution image of AgNPs synthesised at optimised conditions is shown in Fig. 6. It is observed that the size distribution of AgNPs range from 4 to 18 nm. The calculated average particle size of AgNPs is 8 nm. The predicted value for average particle size by model and the obtained value from validation experiment are similar, which confirms the statistical effectiveness of the applied model in optimising the synthesis of AgNPs for minimising the average particle size.

Table 4 Validation of the predicted model using different levels of pH and GA concentration

Run number	pH	GA concentration, mM	Average particle size, nm	
			Predicted	Observed
1	7	6.25	37.87	38.30
2	9	6.25	7.51	8.00
3	11	6.25	37.49	38.00
4	7	7	38.11	37.90
5	9	7	8.34	8.85
6	11	7	38.88	38.95

doi: 10.1049/mnl.2019.0780

To analyse the results of DLS for the synthesised AgNPs, FE-SEM images were investigated. The FE-SEM image corresponds to optimised sample is revealed in Fig. 7. The surface morphology of AgNPs showed even shape and spherical nature. The particle size range from 5 to 20 nm with a narrow size distribution. The obtained average particle size of AgNPs was about 10 nm, which is in good agreement with the observation by DLS. Fig. 8 shows the EDX spectrum of the synthesised AgNPs at optimised conditions, which suggests the presence of Ag as the ingredient element without oxide layer. The quantitative information of AgNPs shows the presence of elements such as Ag (89.75%), oxygen (5.50%), and chlorine (4.75%).

To determine the size, morphology, and dispersity of AgNPs synthesised at optimal conditions, TEM analysis was performed (Fig. 9*a*). The TEM image reveals that the AgNPs formed were spherical in shape and the size of AgNPs was approximately about 4.5–7 nm. The size distribution of NPs was in good agreement with the DLS. A histogram of the size distribution obtained from corresponding TEM image suggests that the average size of the AgNPs was ~5.77 nm and narrow size distribution (Fig. 9*b*).

The UV–vis absorption spectrum of synthesised AgNPs under optimised conditions is shown in Fig. 10. The absorption spectrum

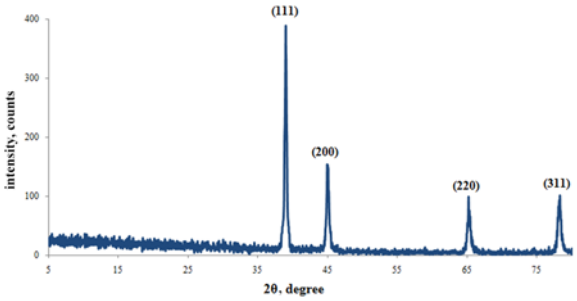

Fig. 5 *XRD pattern of the AgNPs synthesised at optimised conditions*

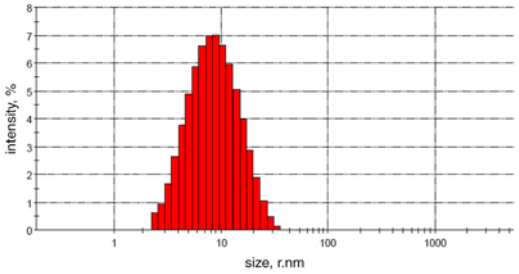

Fig. 6 *DLS analysis of the AgNPs synthesised at optimised conditions*

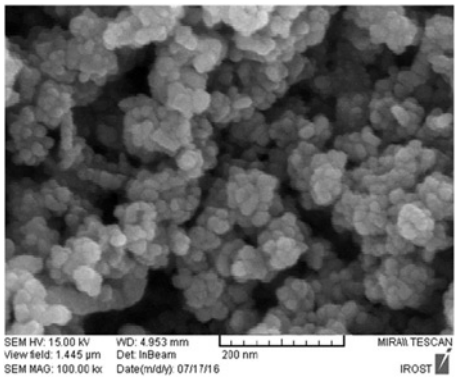

Fig. 7 *FE-SEM image of the AgNPs synthesised at optimised conditions*

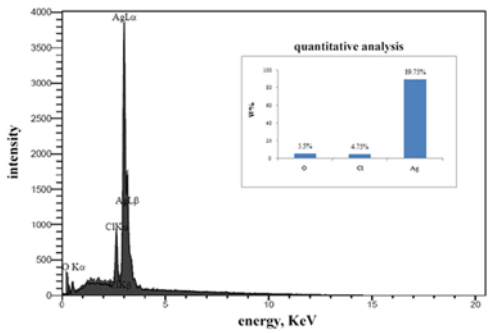

Fig. 8 *EDX spectrum of the AgNPs synthesised at optimised conditions*

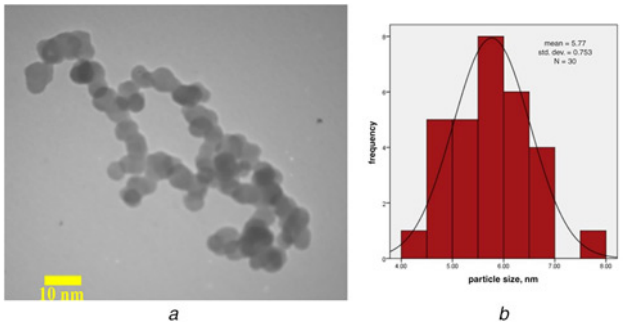

Fig. 9 *TEM analysis*
a TEM image of AgNPs
b Size distribution histogram of AgNPs, synthesised at optimised conditions

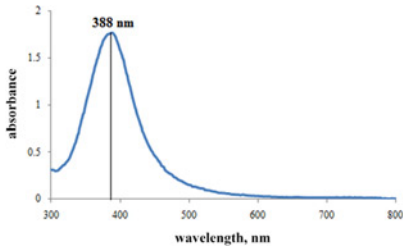

Fig. 10 *UV–vis spectrum of the AgNPs synthesised at optimised conditions*

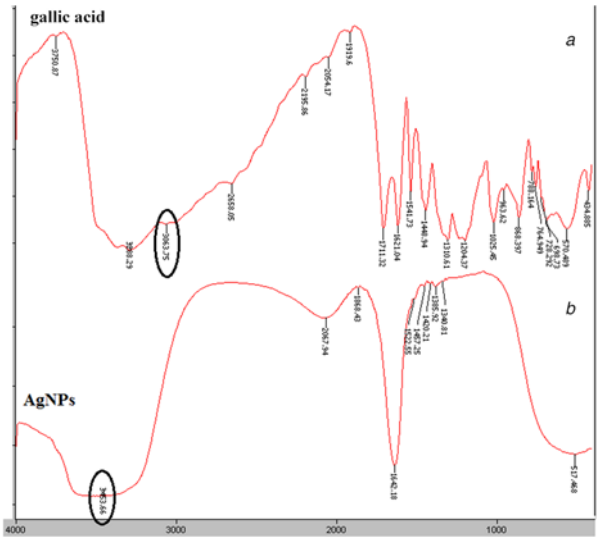

Fig. 11 *FT-IR spectra*
a GA
b AgNPs synthesised at optimised conditions

of NPs showed maximum absorption at 388 nm, which indicates the presence of AgNPs due to the excitation of SPR. The dual role of the GA as a reducing and capping agent was confirmed by FT-IR analysis of AgNPs synthesised at optimal conditions. The FT-IR spectra of the GA and AgNPs are presented in Fig. 11. As previously mentioned, the carboxylic acid groups of GA bind to the surface of the NPs, which was further confirmed by the disappearance of the peak at 3063 cm^{-1} corresponds to the OH stretching vibration of the carboxylic acid groups of GA, which completely disappeared after the synthesis. It validates that carboxylic acid groups in GA have interacted with the AgNPs through electrostatic interactions. The appearance of broad peak at 3453 cm^{-1} for AgNPs confirmed the presence of intermolecular hydrogen-bonded network of phenolic groups on the surface of NPs [30].

4. Conclusion: Our work shows a novel approach including the optimisation of process variables through statistical experimental design for the green synthesis of AgNPs by reduction of $AgNO_3$ with GA as both reducing and capping agent, which have not been already studied by other researchers. The influence of various process factors, namely $AgNO_3$ concentration, GA concentration, and pH in synthesis of AgNPs has been investigated by using RSM based on CCD to determine the optimum synthesis conditions. The results indicate that the pH was the most effective factor on the average particle size in the synthesis process of AgNPs. The AgNPs synthesised at optimised conditions (5.42 mM of $AgNO_3$, 6.25 mM of GA, and pH = 9.02) were investigated through analyses of the DLS, FE-SEM, EDX, UV–vis spectroscopy, and FT-IR. The formation of AgNPs is confirmed by the observed SPR (λ_{max} at 388 nm) in UV–vis absorption spectrum. On the basis of the DLS analysis, the average particle size of AgNPs obtained 8 nm, which was in satisfactory agreement with the predicted value (7.51 nm) by model. The XRD pattern showed the FCC Ag and the average crystallite size of AgNPs was 4.5 nm, estimated from Scherrer method. The analysis of FE-SEM predicts the uniform spherical shape along with the distribution of particle size within the range 5–20 nm. Size distribution histogram obtained from corresponding TEM image reveals that the average size of the AgNPs was ~5.77 nm and narrow size distribution.

5 References

[1] Lundahl P., Stokes R., Smith E., *ET AL.*: 'Synthesis and characterisation of monodispersed silver nanoparticles with controlled size ranges', *Micro Nano Lett.*, 2008, **3**, (2), pp. 62–65

[2] Shenashen M.A., El-Safty S.A., Elshehy E.A.: 'Synthesis, morphological control, and properties of silver nanoparticles in potential applications', *Part. Part. Syst. Charact.*, 2014, **31**, pp. 293–316

[3] Coskun S., Aksoy B., Unalan H.E.: 'Polyol synthesis of silver nanowires: an extensive parametric study', *Cryst. Growth Des.*, 2011, **11**, (11), pp. 4963–4969

[4] Amany A., El-Rab S.F.G., Gad F.: 'Effect of reducing and protecting agents on size of silver nanoparticles and their anti-bacterial activity', *Der Pharma Chem.*, 2012, **4**, (1), pp. 53–65

[5] Nadjari H.Z., Azad A.: 'Determining the non-linear coefficient of gold and silver nano-colloids using SPM and CW Z-scan', *Opt. Laser Technol.*, 2012, **44**, (5), pp. 1629–1632

[6] Perelaer J., Smith P.J., Mager D., *ET AL.*: 'Printed electronics: the challenges involved in printing devices, interconnects, and contacts based on inorganic materials', *J. Mater. Chem.*, 2010, **20**, pp. 8446–8453

[7] Acharya D., Mohanta B., Pandey P., *ET AL.*: 'Optical and antibacterial properties of synthesised silver nanoparticles', *Micro Nano Lett.*, 2017, **12**, (4), pp. 223–226

[8] Pârvulescu V.I., Cojocaru B., Pârvulescu V., *ET AL.*: 'Sol–gel-entrapped nanosilver catalysts – correlation between active silver species and catalytic behavior', *J. Catal.*, 2010, **272**, (1), pp. 92–100

[9] Lee J.B., Park S.J., Kim S.S., *ET AL.*: 'Fabrication of silver stabilization layer of coated conductor using organic silver complexes', *Physica C*, 2010, **470**, (20), pp. 1338–1341

[10] Ma Y., Li N., Yang C., *ET AL.*: 'One-step synthesis of amino-dextran-protected gold and silver nanoparticles and its application in biosensors', *Anal. Bioanal. Chem.*, 2005, **382**, pp. 1044–1048

[11] Keskinen J., Ruuskanen P., Karttunen M., *ET AL.*: 'Synthesis of silver powder using a mechanochemical process', *Appl. Organometallic Chem.*, 2001, **15**, pp. 393–395

[12] Song K.C., Lee S.M., Park T.S., *ET AL.*: 'Preparation of colloidal silver nanoparticles by chemical reduction method', *Korean J. Chem. Eng.*, 2009, **26**, (1), pp. 153–155

[13] Maria B.S., Devadiga A., Kodialbail V.S., *ET AL.*: 'Synthesis of silver nanoparticles using medicinal *Zizyphus xylopyrus* bark extract', *Appl. Nanosci.*, 2015, **5**, (6), pp. 755–762

[14] Ray D., Chatterjee S., Sarkar K., *ET AL.*: 'Silver nanoparticles in hydrogels and microemulsions – a comparative account of their properties and bio-activity', *Mater. Res. Exp.*, 2014, **1**, (3), pp. 035022–035039

[15] Basu S., Maji P., Ganguly J.: 'Rapid green synthesis of silver nanoparticles by aqueous extract of seeds of Nyctanthes arbor-tristis', *Appl. Nanosci.*, 2016, **6**, (1), pp. 1–5

[16] Pourmortazavi S.M., Taghdiri M., Makari V., *ET AL.*: 'Procedure optimization for green synthesis of silver nanoparticles by aqueous extract of *Eucalyptus oleosa*', *Spectrochim. Acta A, Mol. Biomol. Spectrosc.*, 2015, **136**, pp. 1249–1254

[17] Cheviron P., Gouanvé F., Espuche E.: 'Green synthesis of colloid silver nanoparticles and resulting biodegradable starch/silver nanocomposites', *Carbohydr. Polym.*, 2014, **108**, pp. 291–298

[18] Kalaki Z.A., Safaei Javan R., Faraji H.: 'Procedure optimisation for green synthesis of silver nanoparticles by Taguchi method', *Micro Lett.*, 2018, **13**, (4), pp. 558–561

[19] Park J., Cha S.H., Cho S., *ET AL.*: 'Green synthesis of gold and silver nanoparticles using gallic acid: catalytic activity and conversion yield toward the 4-nitrophenol reduction reaction', *J. Nanoparticle Res.*, 2016, **18**, (6), pp. 1–13

[20] Kim D.Y., Kim M., Shinde S., *ET AL.*: 'Cytotoxicity and antibacterial assessment of gallic acid capped gold nanoparticles', *Colloids Surf. B, Biointerfaces*, 2017, **149**, pp. 162–167

[21] Jamdagni P., Khatri P., Rana J.S.: 'Biogenic synthesis of silver nanoparticles from leaf extract of *Elettaria cardamomum* and their antifungal activity against phytopathogens', *Adv. Mater. Process.*, 2018, **3**, (3), pp. 129–135

[22] Marandi R., Khosravi M., Olya M.E., *ET AL.*: 'Photocatalytic degradation of an azo dye using immobilised TiO_2 nanoparticles on polyester support: central composite design approach', *Micro Nano Lett.*, 2011, **6**, (11), pp. 958–963

[23] Balachandran M., Devanathan S., Muraleekrishnan R., *ET AL.*: 'Optimizing properties of nanoclay–nitrile rubber (NBR) composites using face-centred central composite design', *Mater. Des.*, 2012, **35**, pp. 854–862

[24] Ahmadi M., Vahabzadeh F., Bonakdarpour B., *ET AL.*: 'Application of the central composite design and response surface methodology to the advanced treatment of olive oil processing wastewater using Fenton's peroxidation', *J. Hazard. Mater. B*, 2005, **123**, pp. 187–195

[25] Ahani M., Khatibzadeh M.: 'Optimisation of significant parameters through response surface methodology in the synthesis of silver nanoparticles by chemical reduction method', *Micro Nano Lett.*, 2017, **12**, (9), pp. 705–710

[26] Özer A., Gürbüz G., Çalimli A., *ET AL.*: 'Biosorption of copper (II) ions on *Enteromorpha prolifera*: application of response surface methodology (RSM)', *Chem. Eng. J.*, 2009, **146**, (3), pp. 377–387

[27] Djoudi W., Aissani-Benissad F., Bourouina-Bacha S.: 'Optimization of copper cementation process by iron using central composite design experiments', *Chem. Eng. J.*, 2007, **133**, (1–3), pp. 1–6

[28] Njagi E.C., Huang H., Stafford L., *ET AL.*: 'Biosynthesis of iron and silver nanoparticles at room temperature using aqueous sorghum bran extracts', *Langmuir*, 2011, **27**, (1), pp. 264–271

[29] Sathishkumar M., Sneha K., Won S.W., *ET AL.*: '*Cinnamon zeylanicum* bark extract and powder mediated green synthesis of nano-crystalline silver particles and its bactericidal activity', *Colloids Surf. B, Biointerfaces*, 2009, **73**, (2), pp. 332–338

[30] Yoosaf K., Ipe B.I., Suresh C.H., *ET AL.*: '*In situ* synthesis of metal nanoparticles and selective naked-eye detection of lead ions from aqueous media', *J. Phys. Chem. C*, 2007, **111**, (34), pp. 12839–12847

doi: 10.1049/mnl.2019.0780